Science of the Total Environment 819 (2022) 153095

Contents lists available at ScienceDirect

Science of the Total Environment

journal homepage: www.elsevier.com/locate/scitotenv

Chronic exposure to environmentally relevant concentrations of guanylurea induces neurotoxicity of *Danio rerio* adults

Gustavo Axel Elizalde-Velázquez [a], Leobardo Manuel Gómez-Oliván [a,*], Karina Elisa Rosales-Pérez [a], José Manuel Orozco-Hernández [a], Sandra García-Medina [b], Hariz Islas-Flores [a], Marcela Galar-Martínez [b]

[a] Laboratorio de Toxicología Ambiental, Facultad de Química, Universidad Autónoma del Estado de México, Paseo Colón intersección Paseo Tollocan, Colonia Residencial Colón, CP 50120 Toluca, Estado de México, Mexico

[b] Laboratorio de Toxicología Acuática, Departamento de Farmacia, Escuela Nacional de Ciencias Biológicas, Instituto Politécnico Nacional, Unidad Profesional Adolfo López Mateos, Av. Wilfrido Massieu s/n y cerrada Manuel Stampa, Col. Industrial Vallejo, Ciudad de México, CP 07700, Mexico

HIGHLIGHTS

- Guanylurea induces an anxiety-like state in fish after four months of exposure.
- Chronic exposure to guanylurea promotes the production of ROS in the brain.
- Fish exposed to guanylurea showed a significant decrease in acetylcholinesterase activity.
- This metabolite upregulated the expression of p53, BAX, CASP3 in the brain.
- Guanylurea is likely to produce B-amyloid aggregates in the brain as metformin does.

GRAPHICAL ABSTRACT

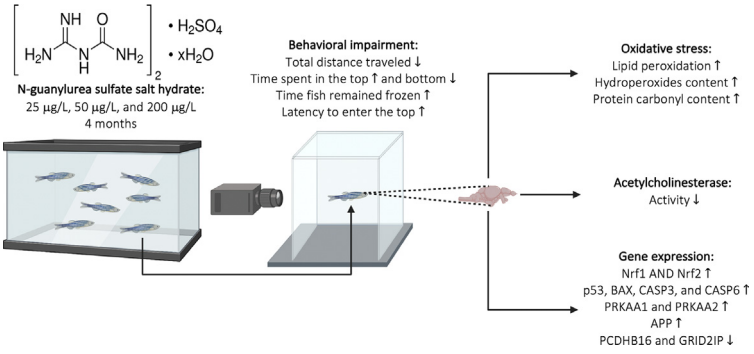

ARTICLE INFO

Article history:
Received 7 December 2021
Received in revised form 7 January 2022
Accepted 9 January 2022
Available online 14 January 2022

Editor: Damia Barcelo

Keywords:
Guanylurea
Neurotoxicology
Behavior
Oxidative stress

ABSTRACT

Recent studies have shown guanylurea (GUA) alters the growth and development of fish, induces oxidative stress, and disrupts the levels and expression of several genes, metabolites, and proteins related to the overall fitness of fish. Nonetheless, up to date, no study has assessed the potential neurotoxic effects that GUA may induce in non-target organisms. To fill the current knowledge gaps about the effects of this metabolite in the central nervous system of fish, we aimed to determine whether or not environmentally relevant concentrations of this metabolite may disrupt the behavior, redox status, AChE activity in *Danio rerio* adults. In addition, we also meant to assess if 25, 50, and 200 μg/L of GUA can alter the expression of several antioxidant defenses-, apoptosis-, AMPK pathway-, and neuronal communication-related genes in the brain of fish exposed for four months to GUA. Our results demonstrated that chronic exposure to GUA altered the swimming behavior of *D. rerio*, as fish remained more time frozen and traveled less distance in the tank compared to the control group. Moreover, this metabolite significantly increased the levels of oxidative damage biomarkers and inhibited the activity of acetylcholinesterase of fish in a concentration-dependent manner. Concerning gene expression, environmentally relevant concentrations of GUA downregulated the expression GRID2IP, PCDH17, and PCDH19, but upregulated Nrf1, Nrf2, p53, BAX, CASP3, PRKAA1, PRKAA2, and APP in fish after four months of exposure. Collectively, we can conclude that GUA may alter the homeostasis of several essential brain biomarkers, generating anxiety-like behavior in fish.

* Corresponding author at: Laboratorio de Toxicología Ambiental, Facultad de Química, Universidad Autónoma del Estado de México, Paseo Colón intersección Paseo Tollocan, Colonia Residencial Colón, CP 50120 Toluca, Estado de México, Mexico.
E-mail address: lmgomezo@uaemex.mx (L.M. Gómez-Oliván).

http://dx.doi.org/10.1016/j.scitotenv.2022.153095

1. Introduction

The first-line oral treatment and the most prescribed oral agent for type II diabetes is metformin (MET) (Elizalde-Velázquez and Gómez-Oliván, 2020). Moreover, in the last decade, different studies have pointed out this drug is efficient against other diseases like the Stein-Leventhal syndrome, cancer, epilepsy, and COVID-19 (Sharma et al., 2020; Vazifehkhah et al., 2020; Zhao et al., 2020; Meng and Zhu, 2021). Thus, MET is among the most consumed drugs all over the world (Ussery et al., 2019), and data point out this consumption is likely to increase as more evidence concerning MET benefits against other diseases emerges.

Once administered, MET is not metabolized and is excreted unchanged from the human body via urine (90%) and feces (Triggle and Ding, 2017), which end up collected in wastewater treatment plants (WWTPs). Even though some studies have indicated WWTPs can eliminate MET from wastewater, the truthfulness is, this drug is only bio-transformed into guanylurea (GUA) by bacteria used in some treatments of these plants (Trautwein et al., 2014; Tisler and Zwiener, 2019). In point of fact, up to date, studies have shown that the only viable method for removal of MET from WWTPs is phytoremediation with *Typha latifolia* (Elizalde-Velázquez and Gómez-Oliván, 2020). Hence, WWTPs often spill out higher concentrations of GUA than those of MET into the aquatic environment (Scheurer et al., 2012; Elliott et al., 2017; Posselt et al., 2018). Recently, GUA has been reported in WWTPs effluents at concentrations of <0.028 μg/L to 810 μg/L and in surface waters at concentrations of 0.001 μg/L to 222 μg/L (Trautwein et al., 2014; Kosma et al., 2015; Tisler and Zwiener, 2018; Posselt et al., 2018; Yao et al., 2018). Nonetheless, as MET consumption is expected to increase due to its usage for non-diabetic indications (Wang et al., 2017), MET and GUA levels in WWTPs effluents and surface waters are also likely to increase.

As a result of its release into the aquatic environment, GUA may exert different toxic effects on water organisms. For instance, Ussery et al. (2019) showed that guanylurea (1–100 ng/L) altered the growth of *Oryzias latipes* after 28 days of exposure. In agreement with these results, Elizalde-Velázquez et al., 2021b demonstrated that GUA (25 μg/L–25 mg/L) delayed the hatching process and induced several malformations through an oxidative stress mechanism on *Danio rerio* embryos after 96 h of exposure. In addition, Ussery et al., 2021 indicated that 28 days of exposure to 1.0 ng/L of GUA altered several metabolites, proteins, and genes related to the overall fitness of *O. latipes*. Among all the genes, metabolites, and proteins that this biotransformation product altered in *O. latipes* larvae, Ussery et al. (2021) indicated that GUA impaired the gene expression of glutamate receptor ionotropic delta-2 interacting protein (Grid2ip) and the abundance of protocadherin beta-16, which may lead to modifications in neuronal communication. Hence, just like its parent compound, to which studies have associated it with B-amyloid formation in the brain of mice (7 days–3 months of exposure) and different neuroblastoma cell cultures (24 h–10 days of exposure) (Chen et al., 2009; Picone et al., 2015; Picone et al., 2016), induction of impaired cognitive function in non-diabetic fish (2 and 4 months of exposure) and mice (1–8 months of exposure) (DiTacchio et al., 2015; MacLaren et al., 2018; Li et al., 2019), and inhibition of AChE activity in healthy humans (Markowicz-Piasecka et al., 2017), GUA is likely to may also exert neurotoxic effects in non-target organisms.

Since GUA is present in the aquatic environment in higher concentrations than its parent compound, no study has assessed the potential neurotoxic effects this metabolite may induce in non-target organisms, and authors have pointed out low concentrations of GUA induces toxic effects in larvae of fish, we aimed to determine whether or not environmentally relevant concentrations of this metabolite may disrupt the behavior, redox status, AChE activity in *D. rerio* adults. Moreover, we also assessed the expression of several antioxidant defenses-, apoptosis-, AMPK pathway-, and neuronal communication-related genes in the brain of fish exposed for four months to GUA. We hypothesize GUA will enter the brain of fish, producing neurotoxic effects on them.

2. Method

2.1. Ethics statement

All procedures performed in this study fulfilled the ethical standards of The Ethics and Research Committee of the Autonomous University of the State of Mexico (approval ID: RP.UAEM.ERC.132.2020).

2.2. Chemicals

N-Guanylurea sulfate salt hydrate (CAS number: 207300-86-5) and all other reagents used in this work were purchased from Sigma-Aldrich (St. Louis, MO).

2.3. Zebrafish maintenance

We housed female and male five-month-old *D. rerio* adults (AB strain, 3.5 ± 0.2 cm, 475 ± 20 mg), in a ratio of 1 organism/L, in aquaria of 100 L (61.2 cm × 32 cm × 51.1 cm). Each aquarium was provided with dechlorinated, charcoal-filtered, and UV-sterilized tap water. To ensure all aquaria fulfilled the water quality parameters throughout the zebrafish maintenance and exposure, we measured the levels of oxygen dissolved, nitrate, nitrite, and un-ionized ammonia in water every other day (Table 1). Moreover, we ensure temperature (27 ± 1 °C) and dark/light cycles (14:10 h) were kept constant along the housing process. Fish were fed two times a day with Spirulina flakes (Ocean Nutrition, US) and supplemented once a day with fresh *Artemia nauplii*.

2.4. Zebrafish exposure

For this experiment, we allocated four systems in aquaria of 30 L of capacity (50 cm × 20 cm × 30 cm), ensuring each system had 15 male and 15 female fish each. We exposed all systems to one of the four GUA treatment concentrations (0 μg/L, 25 μg/L, 50 μg/L, and 200 μg/L). The concentrations used in this experiment were chosen as these range of concentrations have been previously reported in the aquatic environment (Scheurer et al., 2012; Elliott et al., 2017; Posselt et al., 2018; Elizalde-Velázquez and Gómez-Oliván, 2020) and have been shown to induce oxidative damage in *D. rerio* (Elizalde-Velázquez et al., 2021b). Through the four months of exposure, we kept constant the temperature (27 ± 1 °C) and light/dark cycles (14 h:10 h) in all systems. Water from all systems was renewed every other day during all exposure.

2.5. Assessment of swimming behavior

To assess the swimming behavior of *D. rerio* adults, we used the Novel Tank Test described by Cachat et al. (2010) with some modifications. Accordingly, we transferred the fish, together and in their respective aquaria, from the husbandry room to the behavioral room and kept them there for no <50 min. The behavioral room maintained the same temperature conditions as the maintenance room (27 ± 1 °C); however, the behavioral room differs from the latter, as it is soundproof and does not allow light passes. Upon their acclimatization in the behavioral room, we chose one fish at a time and placed it into a 15 L rectangular novel tank (21.2 cm × 21.2 cm × 25.2 cm) for 12 min (2 min of acclimatization, 10 min of trial). Before individual acclimatization and

Table 1
Measured water parameters in aquaria of maintenance and exposure.

Parameters	Measured value
Dissolved oxygen	9.1 ± 0.3 mg/L
Nitrite	0.027 ± 0.009 mg/L
Nitrate	2.9 ± 0.3 mg/L
pH	7.21 ± 0.10
Un-ionized ammonia	0.011 ± 0.003 mg/L

Values are expressed as mean ± standard deviation.

evaluation of fish, we made sure tanks were free of GUA and water had the same temperature and fulfilled the quality conditions described in Section 2.2. Along the trial time, a videotape of each fish was filmed, which then we examined with Tox Track Ink software. Behavioral endpoints measured were the time fish remained frozen in the top and bottom (s), total distance traveled (cm), distance traveled in the top and bottom (cm), latency to enter the top (s), and time spent in the top and bottom (s). To ensure fish did not suffer from any disturbance during the behavioral test, we carried out this test only in the morning (8 am–10 am) and on different days. We performed this experiment three times to calculate the mean of three independent results and then depict them in bar charts (n = 3). Following behavioral assessment, we euthanized fish employing the hypothermic shock method (2–4 °C) and following the AVMA Guidelines on Euthanasia 2020 Edition (Underwood and Anthony, 2020). This method is adequate for this proof, as fish become immobilized instantly upon contact with the cold water, and behavioral markers of pain or distress hardly occur (Wallace et al., 2018). Once fish did not show vital signs, we proceeded to extract the brains of all fish, which we then collected in Eppendorf tubes that we previously had refilled with 1 mL of phosphate buffer solution (PBS, pH 7.4). For brain extraction and dissection, we followed the protocol established by Gupta and Mullins (2010). Briefly, we carefully dried the fish with a paper towel and placed it on a dissecting mat. Next, we removed the head from the rest of the body fish with the help of a scalpel and took off as much soft tissue as possible from the ventral side of the skull with forceps. Following this, we extracted the eyes, placed the head in a dish of PBS, and removed the skin and skull bones from the dorsal and ventral sides of the brain. Finally, we weighted the brains collected for each concentration (76–78 mg).

2.6. Assessment of oxidative stress biomarkers

By using a rotor-stator homogenizer (Ultra-turrax T25, IKA, Germany), we homogenized the brains from each treatment group during 20 s at 10000 rpm and used the homogenate to evaluate all biomarkers. In the case of oxidative stress biomarkers, we opted to use different spectrophotometry methods, see Table 2. For this effect, we treated the samples as Elizalde-Velázquez et al. (2021a,b) described. Briefly, we split up the homogenate into two Eppendorf tubes. Thus, one of the tubes contained 300 μL of trichloroacetic acid (20%) and the same amount of the homogenate, and the other one only enclosed 700 μL of the latter. Finally, we centrifuged tubes 1 and 2 at 11,495 and 12,500 rpm, respectively, and used supernatant and precipitate to evaluate the whole oxidative stress biomarkers battery. Results from all biomarkers were normalized against total proteins by the Bradford (1976). For evaluation of oxidative stress and subsequent biochemical and molecular tests, we analyzed the brains from the three independent experiments we mentioned above, and also for each biomarker, we evaluated the samples three different times. Accordingly, we got nine different results per biomarker and per concentration (n = 9), to which we calculated the mean and standard deviation and represented them in bar charts.

2.7. Assessment of acetylcholinesterase (AChE) activity

For the evaluation of AChE activity, we used the method described by Ellman et al. (1961); so, once we got the homogenate from brains, we centrifuged them at 10000 rpm for 15 min at 4 °C. Next, 400 μL of the supernatant were mixed with 2.6 mL of phosphate buffer (pH 8.0, 0.1 M), 0.1 mL of DTNB (5,5-dithiobis-2-nitrobenzoate, 0.1 M), and 25 μL of substrate (acetylthiocholine iodide 0.075 M). Changes in absorbance were measured at 412 nm and recorded every minute for 5 min. We express our results in enzymatic activity units (mol of substrate per minute).

2.8. RT-qPCR

RNA was isolated from pools of 10 brains from each treatment group by using a RNeasy® kit of Qiagen. To assess the quality of isolation, we determined RNA concentrations through the 260/280 ratio using a spectrophotometer (THERMO Scientific NanoDrop 2000/2000c) and evaluated the purity of samples with agarose (1%) gel electrophoresis. For reverse transcription, we used 1 μg of the total RNA and the QuantiTect® Reverse Transcription Kit under the following conditions: 42 °C for 15 min and 95 °C for 3 min. Our template for RT-qPCR was the cDNA. The genes we assessed during this experiment are related to the parent compound of GUA, metformin (Table 3). To perform each RT-qPCR, we used a Rotor-Gene Q (Qiagen) and 50 μL of a solution containing 0.3 μmol primers, 25 μL 2× SYBER Green QuantiTect® (QIAGEN, Hilden, Germany), and 500 ng of cDNA. Reaction conditions were as follows: 94 °C for 15 s, followed by 35 cycles of 94 °C for 15 s, 60 °C for 30s, and 72 °C for 30s. B-actin was used as a housekeeping gene to normalize all the samples.

2.9. GUA quantification

For water sampling, we weekly gathered a total of 10 mL of water from each system following the protocols established by Elizalde-Velázquez et al. (2021a,b). Brain samples were treated according to the method reported by Łabuzek et al., 2010. Briefly, after *D. rerio* brains were homogenized, these were deproteinized with 400 μL of acetonitrile and 500 μL of methanol added with 57 μmol/L of internal standard. Next, the homogenate was filtered (10 μm strainer) and evaporated to dryness at 45 °C under a nitrogen stream. We then dissolved the samples with 100 μL of the mobile phase and

Table 2
Methods used for oxidative stress biomarkers determination in the brain of *Danio rerio*.

Tube	Biomarker	Reagents	Wavelength	Method used
1	Lipid peroxidation	450 μL Tris-HCl 150 nM 1 mL TCA-TBA	535 nm	Buege and Aust, 1978
	Hydroperoxides content	900 μL mixture ($FeSO_4$, H_2SO_4, dehydroxytoluene butylate, and xylenol orange).	560 nm	Jiang et al., 1992
	Protein carbonyl content	150 μL DNPH/HCl 10 nM 500 μL TCA 1 mL guanidine 6 M	366 nm	Levine et al., 1994
2	Superoxide dismutase	260 μL CO_3 buffer (50 mM Na_2CO_3 and 0.1 mM EDTA) 200 μL adrenaline 30 mM	480 nm	Misra and Fridovich, 1972
	Glutathione peroxidase	290 μL reaction buffer (3.5 mM GSH, 1 mM NaN_3, and 0.12 mM NADPH) 100 μL H_2O_2 20 mM 12 μL GR	340 nm	Gunzler and Flohe, 1985
	Catalase	420 μL isolation buffer (0.3 M sucrose, 1 mM EDTA, 5 mM HEPES, and 5 mM KH_2PO_4) 300 μL H_2O_2 20 mM	240 nm	Radi et al., 1991
	Total protein	300 μL distilled water 1.25 mL Bradford reagent (Coomassie blue, Et-OH 96%, H_3PO_4).	595 nm	Bradford, 1976

TCA-HCl stands for Tris hydrochloride. **TCA-TBA** stands for thiobarbituric-trichloroacetic acid. **DNPH** stands for 2,4-Dinitrophenylhydrazine. **TCA** stands for trichloroacetic acid. **EDTA** stands for Ethylenediaminetetraacetic acid. **NADPH** stands for Nicotinamide adenine dinucleotide phosphate.

Table 3
Genes used for qRT-PCR.

Gene	Forward primer	Reverse primer	Reference
Nrf1	TTT GGT TCC CGA TGA AGA CG	TGA TTA GCG TGA GAC TGA GC	Sant et al., 2017
Nrf2	ACC CAA TAG ATC TAC AGA GC	GGT GTT TGG ACA TCA TCT CG	Sant et al., 2017
BAX	GGC TAT TTC AAC CAG GGT TCC	TGC GAA TCA CCA ATG CTG T	Soares et al., 2017
CASP3	CCG CTG CCC ATC ACT A	ATC CTT TCA CGA CCA TCT	Félix et al., 2018
p53	GCA GCG ATG AGG AGA TCT TT	GGG CTC AGA TGA TTC ACG AT	Lei et al., 2017
PRKAA1	TGT GAG GAC GCA GCA AAA GG	GAG GTA AGA GAA GAG GCC AG	Zang et al., 2019
PRKAA2	CGT CAA GAA GGC AAA GTG GC	TTC TTC CGG CGC ACT CTT AG	Zang et al., 2019
APP	GGT GGA GGT GCC GTC AGA	GGT GGA GGT GCC GTC AGA	Moussavi Nik et al., 2012
GRID2IP	AGC CTT GGT CAG TTC TAT CGG	ACA GCA CCG TGT CGT ATA TG	Mikami et al., 2004
PCDH17	CTG TGT TTG AAC AGC CCT CA	TTG CAC CAT CAG TGG GTT TA	Liu et al., 2015
PCDH19	CAA TGG CGA GGT GGT CTA CT	CAA CTC CAG CGT TTT TAG GG	Liu et al., 2015

Nrf1 stands for Nuclear Respiratory Factor 1. **Nrf2** Nuclear Respiratory Factor 2. **BAX** stands for BCL2 Associated X Protein. **CASP3** stands for Caspase 3. **PRKAA2** stands for Protein Kinase AMP-Activated Catalytic Subunit α 2. **PRKAA1** stands for Protein Kinase AMP-Activated Catalytic Subunit α 1. **APP** stands for Amyloid β Precursor Protein. **GRID2IP** stands for Glutamate Receptor, Ionotropic, δ 2-Interacting Protein 1. **PCDH17** stands for Protocadherin 17. **PCDH19** stands for Protocadherin 19.

centrifuged at 16,000*g* for 15 min. Finally, we injected the obtained supernatant onto the autosampler (50 μL).

Brain and water samples were analyzed on an Agilent 1260 HPLC system coupled to an API 5500 Qtrap MS equipped with a Turbo V Ion spray source. The source parameters were maintained as follows: voltage 5.5 kV; collision gas: medium; temperature 400 °C; desolvation gas flow 500 l/h. We achieved separation by using an Xbridge Phenyl column (150 mm × 2.1 mm, particle size 3.5 μm) and a mobile phase of 5.0 mM of MeOH (eluent A) and 5.0 mM ammonium formate (eluent B). The flow rate was 100 μL/min, and the injection volume was 50 μL. For data acquisition and data processing, we used the Analyst 1.6 software. We performed a five-point calibration curve by spiking ultrapure water with GUA at a concentration ranging from 0 μg/L to 250 μg/L. To confirm the accuracy of the proposed method, we spiked ultrapure water with GUA at three different levels 80%, 100%, and 120%.

2.10. Statistical analysis

The results were expressed as the mean ± standard deviation (SD). Significant differences between the means were measured using a Student Newman Keuls test ($p < 0.05$). A one-way ANOVA test with 95% confidence intervals ($\alpha = 0.05$) was applied to determine the significance of differences between concentrations of oxidative stress biomarkers, acetylcholinesterase activity, and gene expression (Sigma Plot 12.3). The data were tested for homoscedasticity Bartlett test, and normality was verified by Shapiro-Wilk test. To evaluate the degree of a relationship between behavioral, biochemical, and molecular variables, we performed a Pearson correlation considering $p < 0.05$ (R software).

3. Results

3.1. Swimming behavior

Chronic exposure to GUA significantly altered the swimming behavior of *D. rerio* (Fig. 1). As can be seen from Fig. 1, the total distance traveled ($F(3,356) = 189.890$; $p < 0.001$), the distance traveled in the top ($F(3,356) = 551.411$; $p < 0.001$), and time spent in bottom ($F(3,356) = 23.162$; $p < 0.001$) were significantly reduced compared to the control group. Moreover, these behavioral endpoints were decreased in a concentration dependent-manner, showing significant differences between concentrations. In contrast to above endpoints, distance traveled in bottom ($F(3,356) = 121.154$; $p < 0.001$), time spent in top ($F(3,356) = 19.743$; $p < 0.001$), latency to enter the top ($F(3,356) = 212.132$; $p < 0.001$), and the time fish remained frozen in the top ($F(3,356) = 24.351$; $p < 0.001$) and bottom ($F(3,356) = 62.162$; $p < 0.001$) significantly increased compared to the control group. In addition, as concentration increased, the value of these endpoints also increased, showing significant differences between concentrations, except for the time fish remained frozen in the bottom.

3.2. Oxidative stress response

Levels of antioxidant enzymes and oxidative damage biomarkers increased in a concentration-dependent manner. Thus, we were able to see significant differences between concentrations in all oxidative stress biomarkers. Furthermore, from Fig. 2 D–F, it can be seen that enzymatic activity of SOD ($F(3,32) = 35.278$; $p < 0.001$), CAT ($F(3,32) = 30.352$; $p < 0.001$), and GPx ($F(3,32) = 28.525$; $p < 0.001$) displayed a significant increase compared to the control group. Analogously, levels of LPX ($F(3,32) = 31.612$; $p < 0.001$), HPx ($F(3,32) = 33.944$; $p < 0.001$), POx ($F(3,32) = 94.810$; $p < 0.001$ exhibited a significant increase compared to the control group (Fig. 2 A–C). The difference between the levels of the biomarkers at the concentration of 200 μg/L and the other concentrations, including the control group, was so huge that we observed levels of HPX and POX were double or almost double the value of the control group.

3.3. AChE activity

Our results demonstrated that chronic exposure to environmentally relevant concentrations of GUA inhibited the AChE activity in the brain of *D. rerio* (Fig. 3). The inhibition of AChE by GUA showed to be in a concentration-dependent manner; so, we were able to find significant differences between treatment groups. In addition, significant differences between treatment groups and the control group were also observed ($F(3,32) = 106.732$; $p < 0.001$). Compared to the control group, we observed that at the concentration of 50 μg/L and 200 μg/L, the AChE activity was two and three times minor, respectively.

3.4. RT-qPCR

The three environmentally relevant concentrations of GUA altered the expression of antioxidant defense-, apoptosis-, AMPK pathway-, and neuronal communication-related genes (Fig. 4). For example, herein, we demonstrated GUA upregulated the gene expression of Nrf1 ($F(3,32) = 1478.323$; $p < 0.001$) and Nrf2 ($F(3,32) = 1338.290$; $p < 0.001$) in a concentration-dependent manner. Moreover, our results indicated that as concentration increased, the gene expression of p53 ($F(3,32) = 1126.002$; $p < 0.001$), BAX ($F(3,32) = 1667.809$; $p < 0.001$; n = 3), and CASP3 ($F(3,32) = 1093.566$; $p < 0.001$) also increased. Similar to antioxidant defense- and apoptosis-related genes, the expression of PRKAA1 ($F(3,32) = 1005.078$; $p < 0.001$) and PRKAA2 ($F(3,32) = 2316.043$; $p < 0.001$) increased as concentration also did. Concerning neuronal genes, we found GUA downregulated the expression of GRID2IP ($F(3,32) = 1160.149$; $p < 0.001$), PCDH17 ($F(3,32) = 1108.866$; $p < 0.001$), and PCDH19 ($F(3,32) = 1219.588$; $p < 0.001$) and upregulated APP ($F(3,32) = 2292.587$; $p < 0.001$). For all genes, we found significant differences between treatment groups, as well as among treatment groups and the control group.

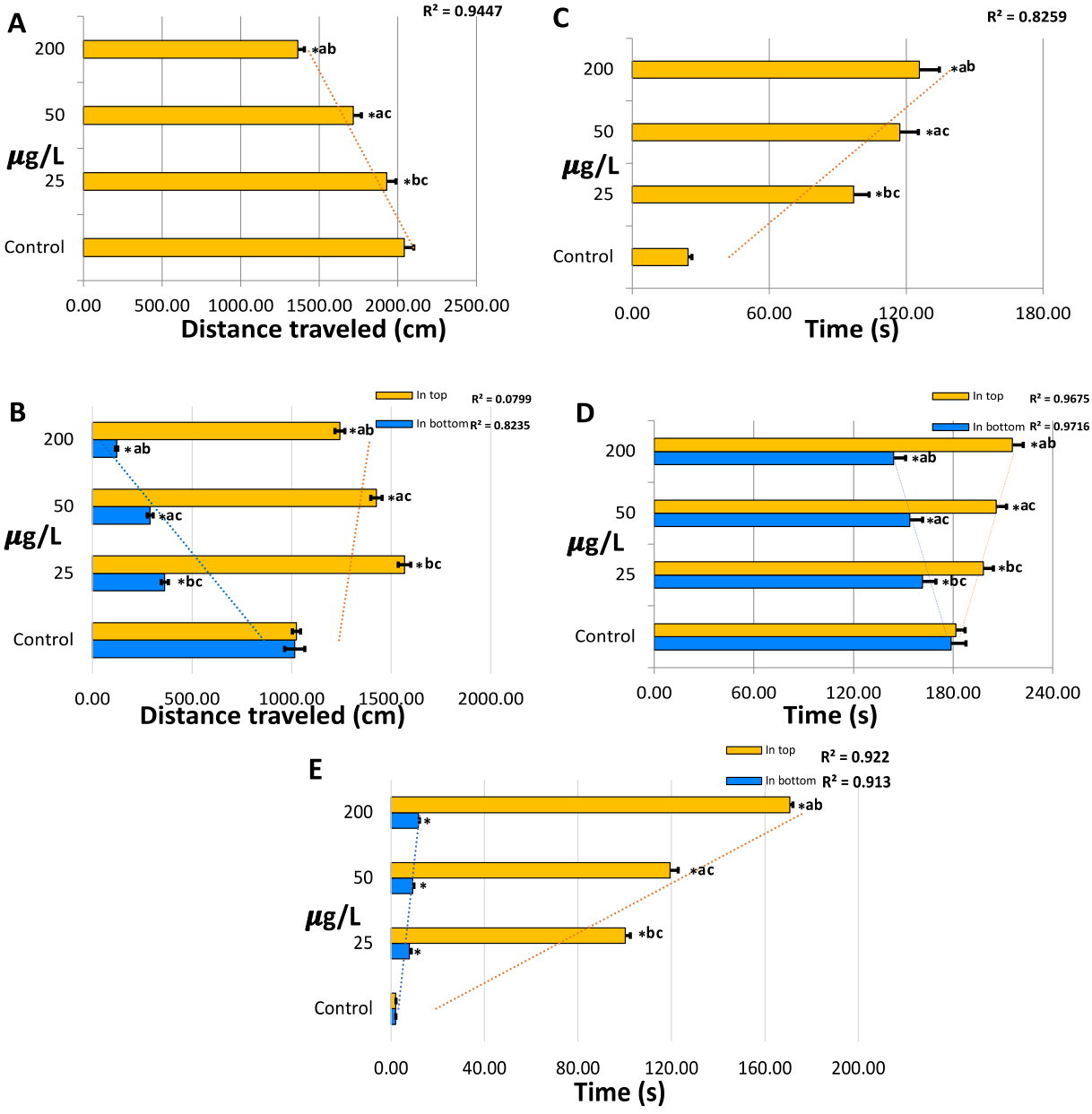

Fig. 1. Alterations to the swimming behavior (total distance traveled **A**, distance traveled in the top and bottom **B**, latency to enter the top **C**, time spent in the top and bottom **D**, and time fish remained frozen in the top and bottom **E**) of *Danio rerio* after chronic exposure to GUA. * denote a significant difference compared to the control group. **a** denote a significant difference compared to 25 µg/L. **b** denote a significant difference compared to 50 µg/L. **c** denote a significant difference compared to 200 µg/L. Data represent mean ± standard deviation of three independent experiments (n = 3).

3.5. GUA concentrations

During all weeks, but 2,8, 12, and 15, we saw the concentration of GUA decrease compared to nominal concentration. The above is because, in those weeks, the day we renewed the water coincided with the day we sampled the water from the medium. For the control group, we found GUA concentrations remained below the limit of quantification during the whole exposure. Since the measured concentrations of GUA did not decrease >20% compared to the nominal concentration, we analyzed all results based on the latter.

Concerning GUA concentrations in the brain, we observed that in all treatment groups, but the control group, GUA levels were above the limit of quantification. Moreover, concentrations of GUA increased in a concentration-dependent manner in all treatment groups. Considering the above data, we calculated the BCF for all concentrations that reached a maximum value of 0.0381 (Tables 4 and 5).

3.6. Pearson correlation

To better understand Fig. 5, it is needed to point out that colors denote the strength of the correlation between variables. Therefore, as the intensity of color increases, the correlation between variables is stronger. In addition, colors also denote the type of correlation; for example, the blue color indicates a positive correlation among variables, while the red color indicates a negative correlation. Our results demonstrated that BCF has a positive correlation to the overproduction of ROS, AChE inhibition, and over-expression of p53, BAX, CASP3, and APP. Moreover, behavioral endpoints related to the distance traveled by fish were positively associated with AChE inhibition and downregulation of GRID2IP, PCDH17, and PCDH19. Meanwhile, those related to the time fish remained frozen were positively correlated to oxidative damage biomarkers and overexpression of apoptosis-related genes.

4. Discussion

Herein, we investigated the potential neurotoxic effects GUA may induce in freshwater fish *D. rerio*. According to our data, GUA impaired the swimming behavior of fish, producing an anxiety-like state in them that fish exhibited by a long-lasting frozen time. Even though our results are the first evidence that GUA impairs the behavior of non-target organisms, previous studies have indicated that the parent compound of this metabolite can disrupt the cognitive function of fish and mice. For example, DiTacchio et al. (2015) and Li et al. (2019) demonstrated that chronic administration of MET to non-diabetic mice at doses that improve insulin sensitivity altered their behavior. Moreover, in fish, MacLaren et al. (2018) pointed out that environmentally relevant concentrations of MET reduced the aggressive behavior of *Betta splendens* adults after one and five months of exposure. We highlight these studies because previous findings have indicated that GUA can mimic the same harmful effects and mechanisms that MET exerts in non-target organisms (Ussery et al., 2019; Ussery et al., 2021; Elizalde-Velázquez et al., 2021b). Therefore, for the data discussed below, we will also consider the information concerning the parent compound of GUA.

Both MET and GUA are related to the production of oxidative stress in fish (Lee et al., 2019; Ussery et al., 2021; Elizalde-Velázquez et al., 2021a,b).

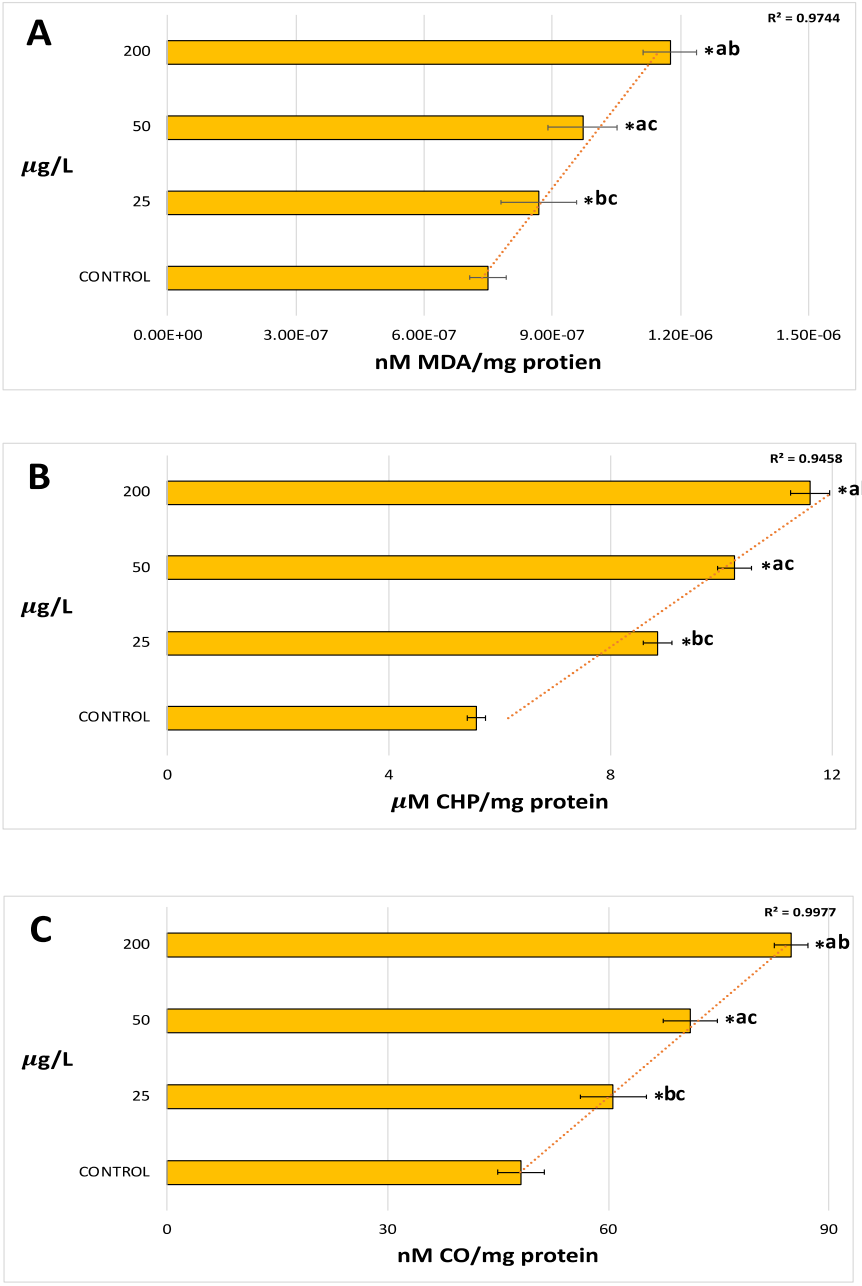

Fig. 2. Oxidative stress response (Lipid peroxidation **A**, Hydroperoxide content **B**, Protein Carbonyl Content **C**, Superoxide Dismutase **D**, Catalase **E**, and Glutathione Peroxidase **F**) of *Danio rerio* after chronic exposure to GUA. * denote a significant difference compared to the control group. **a** denote a significant difference compared to 25 µg/L. **b** denote a significant difference compared to 50 µg/L. **c** denote a significant difference compared to 200 µg/L. Data represent mean ± standard deviation of three independent experiments and three replicas per experiment (n = 9). **MDA** stands for Malondialdehyde. **CHP** stands for Cumene Hydroperoxide. **CO** stands for reactive carbonyls (C = O).

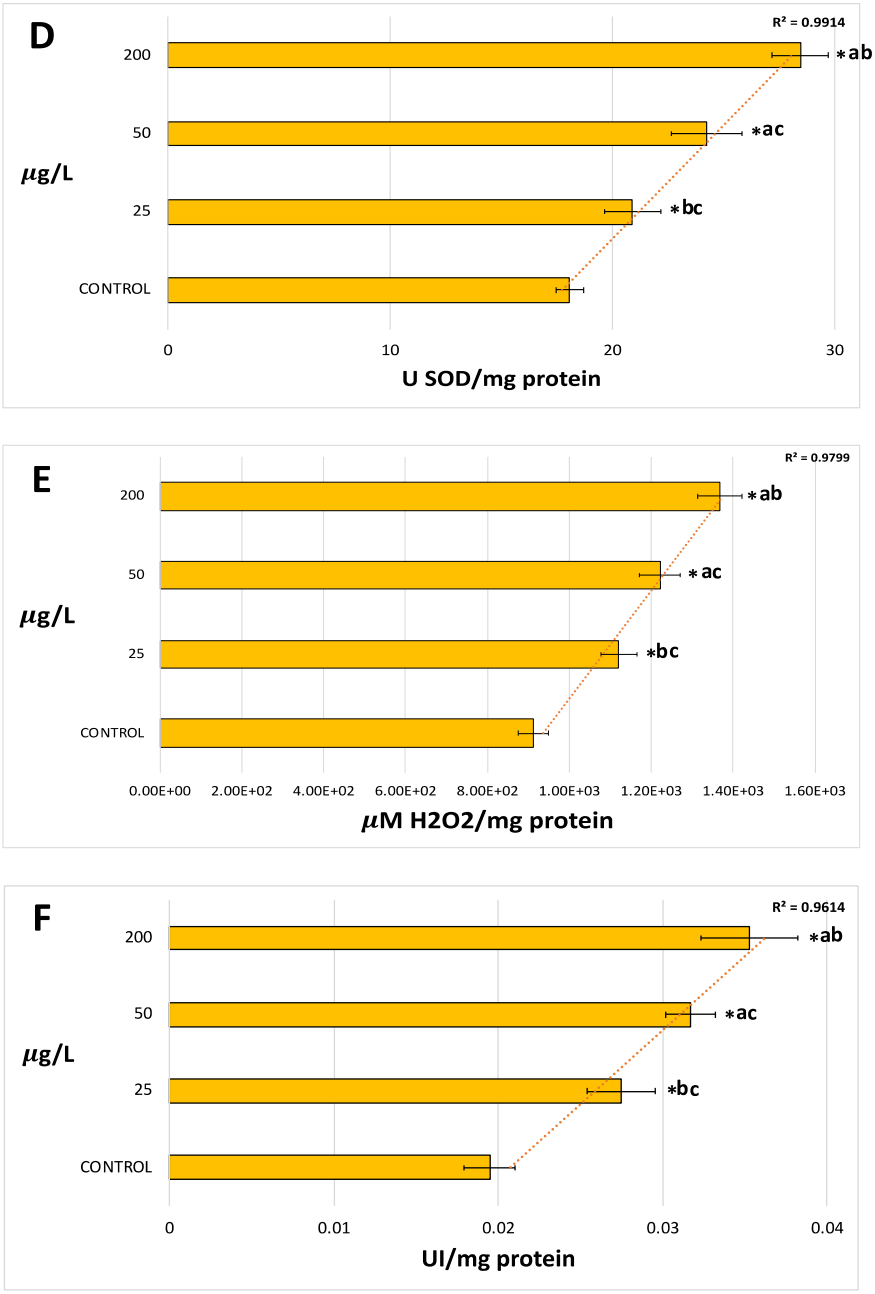

Fig. 2 (*continued*).

In our previous study, for instance, we demonstrated that GUA impaired the redox status of fish, generating several malformations on *D. rerio* embryos (Elizalde-Velázquez et al., 2021b). However, in that study, we did not establish the mechanism by which GUA can produce oxidative stress; instead, we stated that the increased production of ROS in fish was likely due to the mitochondrial impairment that this metabolite might originate. In the present study, we demonstrated that GUA increased the levels of LPX, HPX, and POX in the brain of *D. rerio*. Moreover, our findings also showed GUA upregulated the expression of PRKAA1 and PRKAA2. PRKAA1 and PRKAA2 are the catalytic subunits alpha of the AMP-activated protein kinase (AMPK). AMPK is an important enzyme that regulates the cellular energy status and the activities of several key metabolic enzymes in response to cellular stresses (Ross et al., 2016). In agreement with these results, Ussery et al. (2021), pointed out GUA dysregulated the fatty acids of *Oryzias latipes* larvae via the AMPK pathway. Thus, GUA-induced oxidative stress and its other harmful effects are likely to be induced by the AMPK pathway. Nonetheless, future studies should further study the mechanism by which this metabolite affects the fitness and health of fish.

AMPK activation is not only related to toxic responses in organisms; as a matter of fact, this is the pathway that MET follows to exert its beneficial effects. For example, previous studies have demonstrated MET protects different cellular cultures from oxidative stress by activating Nrf1 via the AMPK (Ashabi et al., 2015; Arbab et al., 2021). In this study, we demonstrated that GUA increased the gene expression of Nrf1 and Nrf2 in fish in a concentration-dependent manner, suggesting that as MET, this metabolite can activate these transcription factors through AMPK. Nonetheless, excessive production of H_2O_2 in cells can also promote the expression Nrf2, as Gureev et al. (2019) stated before. Since in our results, GUA activated the AMPK pathway in a concentration-dependent manner and also increased the production of H_2O_2 in fish, we believe more studies are needed to elucidate the mechanism by which this metabolite upregulated Nrf1 and Nrf2. ROS excessive production is also related to the inhibition of AChE activity.

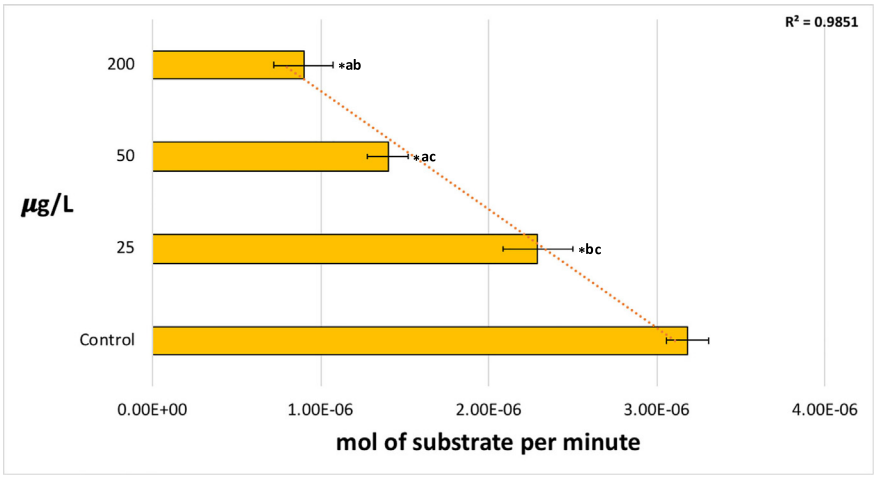

Fig. 3. AChE activity in *Danio rerio* brain after chronic exposure to GUA. * denote a significant difference compared to the control group. **a** denote a significant difference compared to 25 µg/L. **b** denote a significant difference compared to 50 µg/L. **c** denote a significant difference compared to 200 µg/L. Data represent mean ± standard deviation of three independent experiments and three replicas per experiment (n = 9).

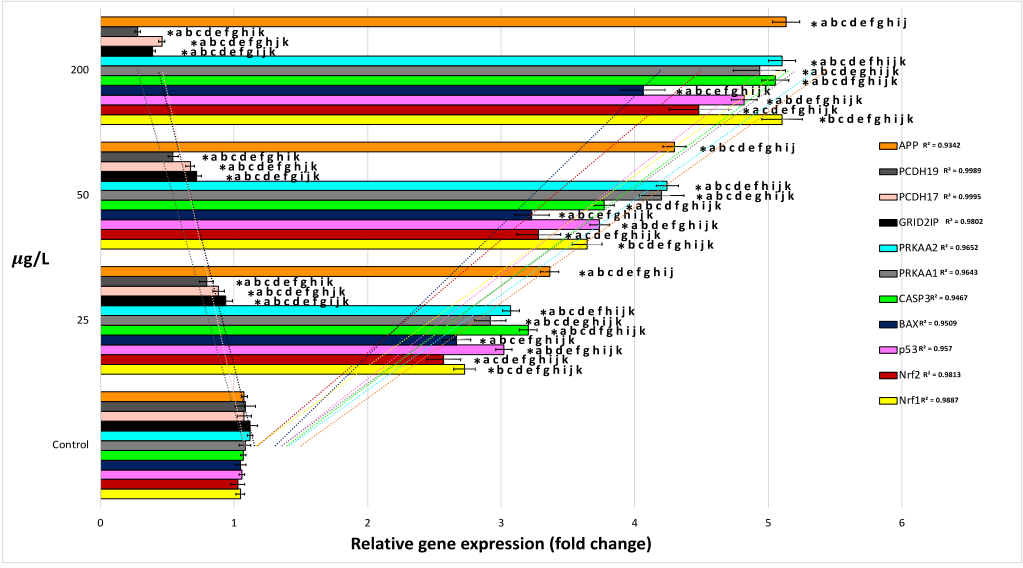

Fig. 4. Expression of antioxidant defense-, apoptosis-, and neuronal communication-related genes of *Danio rerio* after chronic exposure to GUA. * denote a significant difference compared to the control group. **a** denote a significant difference compared to 25 µg/L. **b** denote a significant difference compared to 50 µg/L. **c** denote a significant difference compared to 200 µg/L. Data represent mean ± standard deviation of three independent experiments and three replicas per experiment (n = 9). **APP** stands for Amyloid β Precursor Protein. **PCDH19** stands for Protocadherin 19. **PCDH17** stands for Protocadherin 17. **GRID2IP** stands for Glutamate Receptor, Ionotropic, δ 2-Interacting Protein 1. **PRKAA2** stands for Protein Kinase AMP-Activated Catalytic Subunit α 2. **PRKAA1** stands for Protein Kinase AMP-Activated Catalytic Subunit α 1. **CASP3** stands for Caspase 3. **BAX** stands for BCL2 Associated X Protein. **Nrf1** stands for Nuclear Respiratory Factor 1. **Nrf2** Nuclear Respiratory Factor 2.

Table 4
Measured concentrations of GUA in water samples.

	Nominal concentration	Weeks							
		1	2	3	4	5	6	7	8
Control	ND	<LOQ	<LOQ	<LOQ	<LOQ	<LOQ	<LOQ	<LOQ	<LOQ
GUA	25	22.3 ± 0.8	24.8 ± 0.2	21.8 ± 0.5	21.4 ± 0.7	20.9 ± 0.5	21.0 ± 0.8	20.4 ± 0.5	24.1 ± 0.3
	50	41.7 ± 1.1	48.9 ± 0.8	40.9 ± 1.3	42.1 ± 1.0	41.6 ± 1.2	41.4 ± 1.0	40.7 ± 1.3	48.4 ± 0.6
	200	173.5 ± 6.8	196.3 ± 0.8	168.5 ± 5.7	171.8 ± 6.4	173.1 ± 6.6	169.3 ± 6.2	170.5 ± 7.0	197.8 ± 1.3
	Nominal concentration	Weeks							
		9	10	11	12	13	14	15	16
Control	ND	<LOQ	<LOQ	<LOQ	<LOQ	<LOQ	<LOQ	<LOQ	<LOQ
GUA	25	21.2 ± 0.6	20.5 ± 0.7	21.8 ± 0.6	25.01 ± 0.2	20.9 ± 0.8	21.2 ± 0.7	24.4 ± 0.3	20.9 ± 0.6
	50	41.5 ± 1.2	41.1 ± 1.3	40.4 ± 1.1	48.2 ± 0.8	41.3 ± 1.0	40.5 ± 1.3	48.7 ± 0.5	41.2 ± 1.1
	200	168.3 ± 6.4	170.7 ± 6.1	169.5 ± 5.8	198.6 ± 1.0	169.0 ± 6.2	168.2 ± 7.0	198.2 ± 1.2	169.3 ± 5.9

LOQ: limit of quantification (5 ng/L). LOD: limit of detection (10 ng/L).values are expressed as mean ± standard deviation.

Table 5
Measured concentrations of GUA in brain samples.

Nominal concentration of GUA	Measured concentrations of GUA in the brain of zebrafish
Control	<LOQ
25 μg/L	592 ± 8.1 ng/L
50 μg/L	1219 ± 12.3 ng/L
200 μg/L	6457 ± 10.6 ng/L

LOQ: limit of quantification (8 ng/L). LOD: limit of detection (15 ng/L).

Herein, we demonstrated that GUA led to decreased activity of AChE in fish, which we can explain by the augmented production of H_2O_2. Schallreuter and Elwary (2007), for instance, indicated that this oxidative damage biomarker alters the activity of AChE through the oxidation of several amino acids related to its active center. Moreover, Garcimartín et al. (2017) stated that H_2O_2-induced AChE inhibition is the result of the shifts this biomarker induces in the isoform of the enzyme. Thus, the most likely mechanism by which this metabolite impairs the homeostasis of AChE activity is by excessive production of ROS. However, we did not discard that GUA may also directly inhibit the activity of this enzyme, as previous studies have suggested for its parent compound (Markowicz-Piasecka et al., 2017; Ussery et al., 2018).

AChE activity in the brain is essential for organisms as it regulates neuronal transmission and signaling between synapses by preventing ACh dispersal and activation of nearby receptors (Trang and Khandhar, 2020). Thus, inhibition of this enzyme can lead to physiologic abnormalities extending from behavioral damage to death (Tilton et al., 2011). For example, previous findings have indicated that AChE inhibition is related to the production of convulsions, paralysis, loss of coordination, and other kinds of behavioral changes in organisms (Ren et al., 2015). Moreover, specifically in fish, uncountable studies have related the inhibition of AChE with the generation of anxiety and reduced capacity to escape predation (Qiu et al., 2017; Sandoval-Herrera et al., 2019; Giacomini et al., 2020; Pullaguri et al., 2020). Thus, the behavioral impairment we observed in fish is likely to be the result of GUA-induced AChE inhibition. However, the GUA-induced anxiety behavior in fish can also be a consequence of likely brain damage GUA produced to these organisms. In this study, we found GUA upregulated the gene expression of APP, BAX, p53, and CAPS3. β–Amyloid precursor protein (APP) is a membrane protein that is essential in Alzheimer's disease (AD) pathogenesis (Banote et al., 2020). Cleavage of this membrane protein by beta and gamma secretases generates

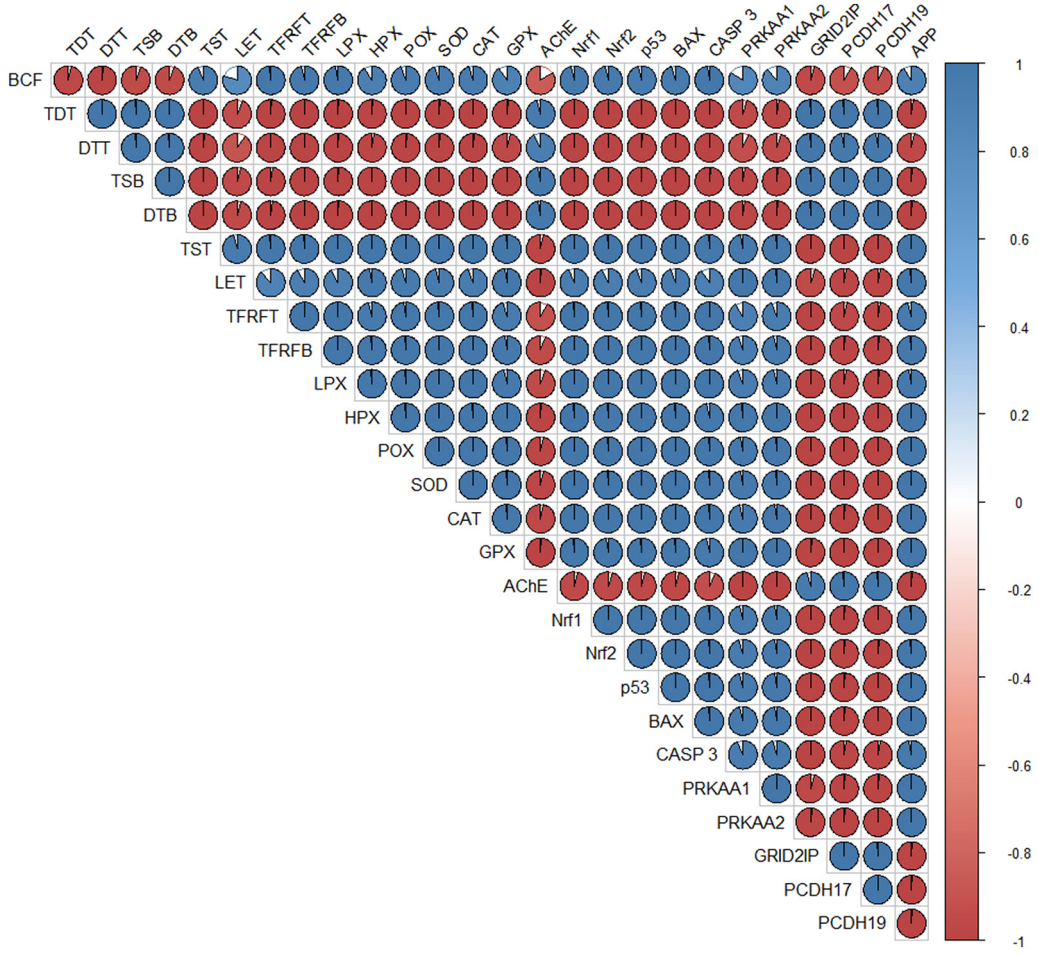

Fig. 5. Pearson's correlation between all variables tested. **BCF** stands for bioconcentration factor. **TDT** stands for total distance traveled. **DTT** stands for distance traveled in the top. **TSB** stands for time spent at the bottom. **DTB** stands for distance traveled in the bottom. **TST** stands for time spent at the top. **LET** stands for latency to enter the top. **TFRFT** stands for time fish remained frozen in the top. **TFRFB** stands for time fish remained frozen in the bottom. **LPX** stands for lipid peroxidation. **HPX** stands for hydroperoxide content. **POX** stands for protein carbonyl content. **SOD** stands for superoxide dismutase. **CAT** stands for catalase. **GPX** stands for glutathione peroxidase. AChE stands for acetylcholinesterase. **Nrf1** stands for Nuclear Respiratory Factor 1. **Nrf2** Nuclear Respiratory Factor 2. **BAX** stands for BCL2 Associated X Protein. **CASP3** stands for Caspase 3. **PRKAA1** stands for Protein Kinase AMP-Activated Catalytic Subunit α 1. **PRKAA2** stands for Protein Kinase AMP-Activated Catalytic Subunit α 2. **GRID2IP** stands for Glutamate Receptor, Ionotropic, δ 2-Interacting Protein 1. **PCDH17** stands for Protocadherin 17. **PCDH19** stands for Protocadherin 19. **APP** stands for Amyloid *β* Precursor Protein.

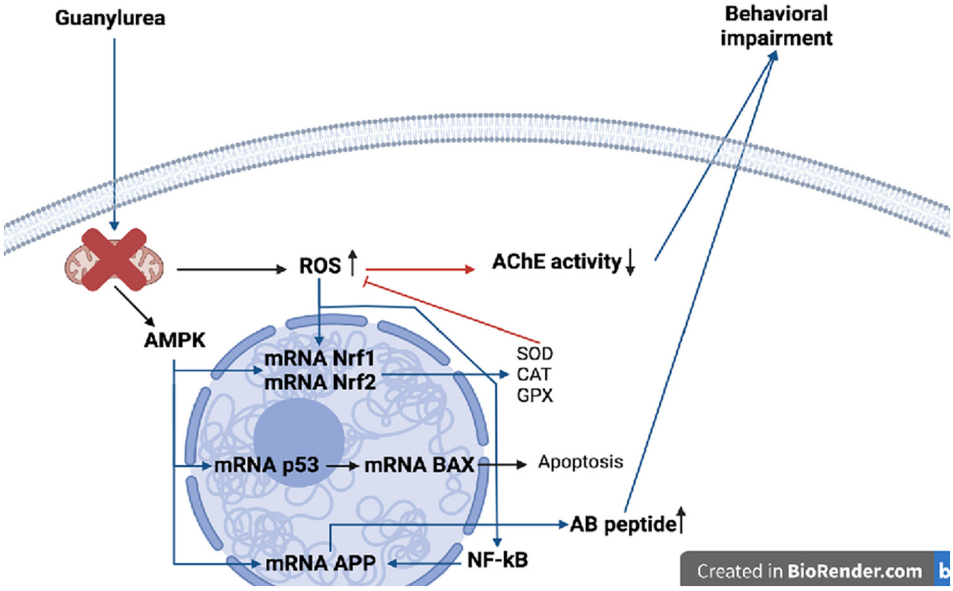

Fig. 6. Potential mechanism by which GUA induces neurotoxicity in fish. GUA crosses the blood-brain barrier and disrupts the homeostasis of mitochondria, which produces an increase in ROS production and the activation of the AMPK pathway. After ROS overproduction in the brain, these can inhibit AChE and/or activate the transcription of APP through the NF-KB pathway and produce behavioral impairment. Moreover, after AMPK activation, it can also activate other transcription factors such as Nrf1 and Nrf2, which counter the overproduction of ROS in the brain, p53, which at the same time activates BAX and induces neuronal apoptosis, and APP that promotes the production of AB peptides and impairs the behavior of fish.

Aβ peptide fragments that aggregate into extracellular plaques in the brain (Selkoe and Hardy, 2016). The over-production and aberrant self-assembly of the amyloid β peptide into fibrillar aggregates is related to neurotoxicity (Karran et al., 2011). Though the mechanism by which the parent compound of GUA promotes the production of β–amyloid is still unknown, studies suggest this can be the result of either AMPK activation or NF-KB induction by ROS (Chen et al., 2009; Picone et al., 2015; Picone et al., 2016). Besides the potential brain damage induced by β–amyloid in GUA exposed fish, apoptosis in the brain of *D. rerio* could also be another possible mechanism by which this metabolite generates neurotoxicity. In agreement with the upregulation of apoptosis-related genes that we observed here, previous studies have shown that MET can augment the protein levels of p53, promote the expression of p21, BAX, and p53, and downregulate the transcription of Bcl2 on different organs of zebrafish and cell cultures (Li et al., 2015; Sharma and Kumar, 2018; Lin et al., 2020). Moreover, Wang et al. (2008) and Koagouw et al. (2021) demonstrated MET induces apoptosis in pancreatic cells and the gonads of *Mytilus edulis*. So far, we have demonstrated that GUA at environmentally relevant concentrations can impair the behavior of fish; however, there is a lot of research to do to understand the mechanisms by which this metabolite produces oxidative stress, AChE inhibition, β–amyloid formation, and apoptosis in fish. Moreover, we also believe that future studies need to evaluate the likely histopathological damage GUA generates in the brain of non-target organisms.

Neurotoxic effects above-described are the result of GUA capacity of crossing the blood-brain barrier (BBB). Herein, for instance, we demonstrated GUA crossed this barrier in a concentration-dependent manner, reaching a BCF of up to 0.0381. Thus, once GUA crosses the BBB, it can activate the AMPK pathway and trigger a neurotoxic response in organisms, characterized by a disruption of redox status, AChE activity, and gene expression. In Fig. 6, we depicted the potential mechanism by which GUA may induce neurotoxicity in fish. Blue arrows indicate a positive correlation, and red arrows a negative one.

5. Conclusions

Danio rerio adults exposed to GUA showed a significant increase in the time they remained frozen and a decrease in the total distance they swam compared to the control group. Freezing of fish may be related to the inhibition of AChE that GUA induced in fish, which is likely to be the result of the oxidative stress response that this metabolite also produced in the brain of this freshwater organism. Impaired behavior of fish could also be related to the capacity of GUA to induce apoptosis, B-amyloid formation, or decrease the abundance of neurotransmitter GRID 2IP and protocadherin in the brain of water organisms, as our results highlighted. Nonetheless, future studies should investigate the histopathological damage this metabolite may induce in the brain of fish. To the best of our knowledge, our results provide the first evidence of neurotoxic effects in fish exposed to environmentally relevant concentrations of GUA.

CRediT authorship contribution statement

GAEV, KERP, JMOH performed all the exposure experiments; LMGO and GAEV were involved in the conception; LMGO and GAEV were involved in the design and interpretation of the data and the writing of the manuscript with input from SGM, HIF and MGM.

Declaration of competing interest

The authors declare that they have no known competing financial interests or personal relationships that could have appeared to influence the work reported in this paper.

Acknowledgements

This study was made possible by financial support from the Consejo Nacional de Ciencia y Tecnología (CONACyT, Project 300727).

References

Arbab, A.A.I., Lu, X., Abdalla, I.M., Idris, A.A., Chen, Z., Li, M., ... Yang, Z., 2021. Metformin inhibits lipoteichoic acid–induced oxidative stress and inflammation through AMPK/NRF2/NF-κB signaling pathway in bovine mammary epithelial cells. Front. Vet. Sci. *8*.

Ashabi, G., Khalaj, L., Khodagholi, F., Goudarzvand, M., Sarkaki, A., 2015. Pre-treatment with metformin activates Nrf2 antioxidant pathways and inhibits inflammatory responses through induction of AMPK after transient global cerebral ischemia. Metab. Brain Dis. 30 (3), 747–754.

Banote, R.K., Chebli, J., Şatır, T.M., Varshney, G.K., Camacho, R., Ledin, J., ... Zetterberg, H., 2020. Amyloid precursor protein-b facilitates cell adhesion during early development in zebrafish. Sci. Rep. 10 (1), 1–16.

Bradford, M.M., 1976. A rapid and sensitive method for the quantitation of microgram quantities of protein utilizing the principle of protein dye binding. Anal. Biochem. 72, 248–254.

Buege, J.A., Aust, S.D., 1978. Microsomal lipid peroxidation. Methods Enzymol. https://doi.org/10.1016/S0076-6879(78)52032-6.

Cachat, J., Stewart, A., Grossman, L., Gaikwad, S., Kadri, F., Chung, K.M., ... Kalueff, A.V., 2010. Measuring behavioral and endocrine responses to novelty stress in adult zebrafish. Nat. Protoc. 5 (11), 1786–1799.

Chen, Y., Zhou, K., Wang, R., Liu, Y., Kwak, Y.D., Ma, T., ... Liao, F.F., 2009. Antidiabetic drug metformin (GlucophageR) increases biogenesis of Alzheimer's amyloid peptides via up-regulating BACE1 transcription. Proc. Natl. Acad. Sci. 106 (10), 3907–3912.

DiTacchio, K.A., Heinemann, S.F., Dziewczapolski, G., 2015. Metformin treatment alters memory function in a mouse model of Alzheimer's disease. J. Alzheimers Dis. 44 (1), 43–48.

Elizalde-Velázquez, G.A., Gómez-Oliván, L.M., 2020. Occurrence, toxic effects and removal of metformin in the aquatic environments in the world: recent trends and perspectives. Sci. Total Environ. 702, 134924.

Elizalde-Velázquez, G.A., Gómez-Oliván, L.M., García-Medina, S., Islas-Flores, H., Hernández-Navarro, M.D., Galar-Martínez, M., 2021a. Antidiabetic drug metformin disrupts the embryogenesis in zebrafish through an oxidative stress mechanism. Chemosphere 285, 131213.

Elizalde-Velázquez, G.A., Gómez-Oliván, L.M., Islas-Flores, H., Hernández-Navarro, M.D., García-Medina, S., Galar-Martínez, M., 2021b. Oxidative stress as a potential mechanism by which guanylurea disrupts the embryogenesis of Danio rerio. Sci. Total Environ. 799, 149432.

Elliott, S.M., Brigham, M.E., Lee, K.E., Banda, J.A., Choy, S.J., Gefell, D.J., ... Jorgenson, Z.G., 2017. Contaminants of emerging concern in tributaries to the Laurentian Great Lakes: I. Patterns of occurrence. PLoS One *12* (9) e0182868.

Ellman, G.L., Courtney, K.D., Andres Jr., V., Featherstone, R.M., 1961. A new and rapid colorimetric determination of acetylcholinesterase activity. Biochem. Pharmacol. 7 (2), 88–95.

Félix, L.M., Vidal, A.M., Serafim, C., Valentim, A.M., Antunes, L.M., Monteiro, S.M., ... Coimbra, A.M., 2018. Ketamine induction of p53-dependent apoptosis and oxidative stress in zebrafish (Danio rerio) embryos. Chemosphere 201, 730–739.

Garcimartín, A., López-Oliva, M.E., González, M.P., Sánchez-Muniz, F.J., Benedí, J., 2017. Hydrogen peroxide modifies both activity and isoforms of acetylcholinesterase in human neuroblastoma SH-SY5Y cells. Redox Biol. 12, 719–726.

Giacomini, A.C., Bueno, B.W., Marcon, L., Scolari, N., Genario, R., Demin, K.A., ... de Abreu, M.S., 2020. An acetylcholinesterase inhibitor, donepezil, increases anxiety and cortisol levels in adult zebrafish. J. Psychopharmacol. 34 (12), 1449–1456.

Gunzler, W., Flohe, L., 1985. Handbook of Methods for Oxygen Radical Research.

Gupta, T., Mullins, M.C., 2010. Dissection of organs from the adult zebrafish. J. Vis. Exp. 37.

Gureev, A.P., Shaforostova, E.A., Popov, V.N., 2019. Regulation of mitochondrial biogenesis as a way for active longevity: interaction between the Nrf2 and PGC-1α signaling pathways. Front. Genet. 10, 435.

Jiang, Z.Y., Hunt, J.V., Wolff, S.P., 1992. Ferrous ion oxidation in the presence of xylenol orange for detection of lipid hydroperoxide in low density lipoprotein. Anal. Biochem. https://doi.org/10.1016/0003-2697(92)90122-N.

Karran, E., Mercken, M., De Strooper, B., 2011. The amyloid cascade hypothesis for Alzheimer's disease: an appraisal for the development of therapeutics. Nat. Rev. Drug Discov. 10, 698–712.

Koagouw, W., Hazell, R.J., Ciocan, C., 2021. Induction of apoptosis in the gonads of Mytilus edulis by metformin and increased temperature, via regulation of HSP70, CASP8, BCL2 and FAS. Mar. Pollut. Bull. 173, 113011.

Kosma, C.I., Lambropoulou, D.A., Albanis, T.A., 2015. Comprehensive study of the antidiabetic drug metformin and its transformation product guanylurea in Greek wastewaters. Water Res. 70, 436–448.

Lee, J.W., Shin, Y.J., Kim, H., Kim, H., Kim, J., Min, S.A., ... Park, K., 2019. Metformin-induced endocrine disruption and oxidative stress of Oryzias latipes on two-generational condition. J. Hazard. Mater. 367, 171–181.

Lei, L., Yan, S.-Y., Yang, R., Chen, J.-Y., Li, Y., Bu, Y., et al., 2017. Spliceosomal protein eftud2 mutation leads to p53-dependent apoptosis in zebrafish neural progenitors. Nucleic Acids Res. 45 (6), 3422–3436. https://doi.org/10.1093/nar/gkw1043.

Levine, R.L., Williams, J.A., Stadtman, E.P., Shacter, E., 1994. Carbonyl assays for determination of oxidatively modified proteins. Methods Enzymol. https://doi.org/10.1016/S0076-6879(94)33040-9.

Li, W., Chaudhari, K., Shetty, R., Winters, A., Gao, X., Hu, Z., ... Yang, S.H., 2019. Metformin alters locomotor and cognitive function and brain metabolism in normoglycemic mice. Aging Dis. 10 (5), 949.

Li, P., Zhao, M., Parris, A.B., Feng, X., Yang, X., 2015. p53 is required for metformin-induced growth inhibition, senescence and apoptosis in breast cancer cells. Biochem. Biophys. Res. Commun. 464 (4), 1267–1274.

Lin, W., Yan, Y., Ping, S., Li, P., Li, D., Hu, J., Rea, Y., 2020. Metformin-induced epigenetic toxicity in zebrafish: experimental and molecular dynamics simulation studies. Environ. Sci. Technol. 55 (3), 1672–1681.

Liu, Q., Bhattarai, S., Wang, N., Sochacka-Marlowe, A., 2015. Differential expression of protocadherin-19, protocadherin-17, and cadherin-6 in adult zebrafish brain. J. Comp. Neurol. 523 (9), 1419–1442.

MacLaren, R.D., Wisniewski, K., MacLaren, C., 2018. Environmental concentrations of metformin exposure affect aggressive behavior in the Siamese fighting fish, Betta splendens. PLoS One 13 (5), e0197259.

Markowicz-Piasecka, M., Sikora, J., Mateusiak, Ł., Mikiciuk-Olasik, E., Huttunen, K.M., 2017. Metformin and its sulfenamide prodrugs inhibit human cholinesterase activity. Oxidative Med. Cell. Longev. 2017.

Meng, J., Zhu, Y., 2021. Efficacy of simvastatin plus metformin for polycystic ovary syndrome: a meta-analysis of randomized controlled trials. Eur. J. Obstet. Gynecol. Reprod. Biol. 257, 19–24.

Mikami, Y., Yoshida, T., Matsuda, N., Mishina, M., 2004. Expression of zebrafish glutamate receptor δ2 in neurons with cerebellum-like wiring. Biochem. Biophys. Res. Commun. 322 (1), 168–176.

Misra, H.P., Fridovich, I., 1972. The role of superoxide anion in the autoxidation of epinephrine and a simple assay for superoxide dismutase. J. Biol. Chem. https://doi.org/10.1016/S0021-9258(19)45228-9.

Moussavi Nik, S.H., Wilson, L., Newman, M., Croft, K., Mori, T.A., Musgrave, I., Lardelli, M., 2012. The BACE1-PSEN-AβPP regulatory axis has an ancient role in response to low oxygen/oxidative stress. J. Alzheimers Dis. 28 (3), 515–530.

Picone, P., Nuzzo, D., Caruana, L., Messina, E., Barera, A., Vasto, S., Di Carlo, M., 2015. Metformin increases APP expression and processing via oxidative stress, mitochondrial dysfunction and NF-κB activation: use of insulin to attenuate metformin's effect. Biochim. Biophys. Acta Mol. Cell Res. 1853 (5), 1046–1059.

Picone, P., Vilasi, S., Librizzi, F., Contardi, M., Nuzzo, D., Caruana, L., ... Di Carlo, M., 2016. Biological and biophysics aspects of metformin-induced effects: cortex mitochondrial dysfunction and promotion of toxic amyloid pre-fibrillar aggregates. Aging (Albany NY) 8 (8), 1718.

Posselt, M., Jaeger, A., Schaper, J.L., Radke, M., Benskin, J.P., 2018. Determination of polar organic micropollutants in surface and pore water by high-resolution sampling-direct injection-ultra high performance liquid chromatography-tandem mass spectrometry. Environ. Sci. Process. Impacts 20 (12), 1716–1727.

Pullaguri, N., Nema, S., Bhargava, Y., Bhargava, A., 2020. Triclosan alters adult zebrafish behavior and targets acetylcholinesterase activity and expression. Environ. Toxicol. Pharmacol. 75, 103311.

Qiu, X., Nomichi, S., Chen, K., Honda, M., Kang, I.J., Shimasaki, Y., Oshima, Y., 2017. Short-term and persistent impacts on behaviors related to locomotion, anxiety, and startle responses of Japanese medaka (Oryzias latipes) induced by acute, sublethal exposure to chlorpyrifos. Aquat. Toxicol. 192, 148–154.

Radi, R., Turrens, J.F., Chang, L.Y., Bush, K.M., Crapo, J.D., et al., 1991. Detection of catalase in rat heart mitochondria. J. Biol. Chem. https://doi.org/10.1016/S0021-9258(18)54740-2.

Ren, Z., Zhang, X., Wang, X., Qi, P., Zhang, B., Zeng, Y., ... Miao, M., 2015. AChE inhibition: one dominant factor for swimming behavior changes of Daphnia magna under DDVP exposure. Chemosphere 120, 252–257.

Ross, F.A., MacKintosh, C., Hardie, D.G., 2016. AMP-activated protein kinase: a cellular energy sensor that comes in 12 flavours. FEBS J. 283 (16), 2987–3001.

Sandoval-Herrera, N., Mena, F., Espinoza, M., Romero, A., 2019. Neurotoxicity of organophosphate pesticides could reduce the ability of fish to escape predation under low doses of exposure. Sci. Rep. 9 (1), 1–11.

Sant, K.E., Hansen, J.M., Williams, L.M., Tran, N.L., Goldstone, J.V., Stegeman, J.J., ... Timme-Laragy, A., 2017. The role of Nrf1 and Nrf2 in the regulation of glutathione and redox dynamics in the developing zebrafish embryo. Redox Biol. 13, 207–218.

Schallreuter, K.U., Elwary, S., 2007. Hydrogen peroxide regulates the cholinergic signal in a concentration dependent manner. Life Sci. 80 (24–25), 2221–2226.

Scheurer, M., Michel, A., Brauch, H.J., Ruck, W., Sacher, F., 2012. Occurrence and fate of the antidiabetic drug metformin and its metabolite guanylurea in the environment and during drinking water treatment. Water Res. 46 (15), 4790–4802.

Selkoe, D.J., Hardy, J., 2016. The amyloid hypothesis of Alzheimer's disease at 25 years. EMBO Mol. Med. 8 (6), 595–608.

Sharma, P., Kumar, S., 2018. Metformin inhibits human breast cancer cell growth by promoting apoptosis via a ROS-independent pathway involving mitochondrial dysfunction: pivotal role of superoxide dismutase (SOD). Cell. Oncol. 41 (6), 637–650.

Sharma, S., Ray, A., Sadasivam, B., 2020. Metformin in COVID-19: a possible role beyond diabetes. Diabetes Res. Clin. Pract. 164, 108183.

Soares, J., et al., 2017. 17 α -ethynilestradiol and tributyltin mixtures modulates the expression of NER and p53 DNA repair pathways in male zebra fi sh gonads and disrupt o ff spring embryonic development. Ecol. Indic. (December 2016), 1–11 https://doi.org/10.1016/j.ecolind.2017.04.054.

Tilton, F.A., Bammler, T.K., Gallagher, E.P., 2011. Swimming impairment and acetylcholinesterase inhibition in zebrafish exposed to copper or chlorpyrifos separately, or as mixtures. Comp. Biochem. Physiol. C Toxicol. Pharmacol. 153 (1), 9–16.

Tisler, S., Zwiener, C., 2018. Formation and occurrence of transformation products of metformin in wastewater and surface water. Sci. Total Environ. 628, 1121–1129.

Tisler, S., Zwiener, C., 2019. Aerobic and anaerobic formation and biodegradation of guanyl urea and other transformation products of metformin. Water Res. 149, 130–135.

Trang, A., Khandhar, P.B., 2020. Physiology, acetylcholinesterase. StatPearls [Internet].

Trautwein, C., Berset, J.D., Wolschke, H., Kümmerer, K., 2014. Occurrence of the antidiabetic drug Metformin and its ultimate transformation product Guanylurea in several compartments of the aquatic cycle. Environ. Int. 70, 203–212.

Triggle, C.R., Ding, H., 2017. Metformin is not just an antihyperglycaemic drug but also has protective effects on the vascular endothelium. Acta Physiol. 219 (1), 138–151.

Underwood, W., Anthony, R., 2020. AVMA guidelines for the euthanasia of animals: 2020 edition. Retrieved on March 2013 (30), 2020–2021.

Ussery, E., Bridges, K.N., Pandelides, Z., Kirkwood, A.E., Bonetta, D., Venables, B.J., ... Holdway, D., 2018. Effects of environmentally relevant metformin exposure on Japanese medaka (Oryzias latipes). Aquat. Toxicol. 205, 58–65.

Ussery, E., Bridges, K.N., Pandelides, Z., Kirkwood, A.E., Guchardi, J., Holdway, D., 2019. Developmental and full-life cycle exposures to guanylurea, and guanylurea-metformin mixtures results in adverse effects on Japanese medaka (*Oryzias latipes*). Environ. Toxicol. Chem. 38 (5), 1023–1028. https://doi.org/10.1002/etc.4403.

Ussery, E.J., Nielsen, K.M., Simmons, D., Pandelides, Z., Mansfield, C., Holdway, D., 2021. An 'omics approach to investigate the growth effects of environmentally relevant

concentrations of guanylurea exposure on Japanese medaka (Oryzias latipes). Aquat. Toxicol. 232, 105761.
Vazifehkhah, S., Khanizadeh, A.M., Mojarad, T.B., Nikbakht, F., 2020. The possible role of progranulin on anti-inflammatory effects of metformin in temporal lobe epilepsy. J. Chem. Neuroanat. 109, 101849.
Wallace, C.K., Bright, L.A., Marx, J.O., Andersen, R.P., Mullins, M.C., Carty, A.J., 2018. Effectiveness of rapid cooling as a method of euthanasia for young zebrafish (Danio rerio). J. Am. Assoc. Lab. Anim. Sci. 57 (1), 58–63.
Wang, Y.W., He, S.J., Feng, X., Cheng, J., Luo, Y.T., Tian, L., Huang, Q., 2017. Metformin: a review of its potential indications. Drug Des. Devel. Ther. 11, 2421.
Wang, L.W., Li, Z.S., You, D.W., Jin, Z.D., Gao, J., Xu, G.M., 2008. Metformin induces apoptosis of pancreatic cancer cells. World J. Gastroenterol. 14 (47), 7192.
Yao, B., Yan, S., Lian, L., Yang, X., Wan, C., Dong, H., Song, W., 2018. Occurrence and indicators of pharmaceuticals in Chinese streams: a nationwide study. Environ. Pollut. 236, 889–898.
Zang, L., Shimada, Y., Nakayama, H., Kim, Y., Chu, D.C., Juneja, L.R., ... Nishimura, N., 2019. RNA-seq based transcriptome analysis of the anti-obesity effect of green tea extract using zebrafish obesity models. Molecules 24 (18), 3256.
Zhao, B., Luo, J., Yu, T., Zhou, L., Lv, H., Shang, P., 2020. Anticancer mechanisms of metformin: a review of the current evidence. Life Sci. 254, 117717.